Optimization of control source locations in free-field active noise control using a genetic algorithm

Connor R. Duke[a], Scott D. Sommerfeldt[b], Kent L. Gee[c] and Cole V. Duke[d]

(Received: 18 September 2008; Revised: 20 January 2009; Accepted: 22 January 2009)

Control source locations in active noise control applications introduce a physical limit in the amount of attenuation achievable by the system. A genetic algorithm was developed to find the optimal control source locations for a primary source configuration in a free-field with a specified number of control sources. The optimal configuration of control sources around a single monopole primary source was shown to be a linear arrangement of the sources. This holds true for both two-dimensional as well as three-dimensional configurations. These results are presented for configurations using up to six control sources. The linear arrangement of control sources provides higher-order radiation characteristics than previously studied arrangements. Experimental verification has shown that a monopole primary source is controlled more effectively with a linear array of sources than sources surrounding the primary source for a broad frequency range. The source strength required from the control sources in each configuration is also explored. ***© 2009 Institute of Noise Control Engineering.***

Primary subject classification: 38.3; Secondary subject classification: 74.3

1 INTRODUCTION

Although active noise control (ANC) in free-field applications has been successfully demonstrated, recent studies have focused on improvement of control system performance through optimization of system parameters[1–5]. Optimization of an ANC system can include (1) control actuator configuration, (2) error sensor placement, (3) reference signal quality, and (4) the controller hardware and software[6]. Of these, the achievable reduction in noise for ANC applications is physically limited[7–11] by the control source configuration, regardless of optimization of other parameters. Optimization of error sensor locations, reference signal, and controller will be futile if the system is limited by the control source arrangement. Studies have been performed by Cunefare, et al. and Elliot and Johnson to understand the recommended number of control sources[12,13]. Based on the assumption that the number of control sources is fixed, optimization of control source location is the focus of this paper.

[a] 745 Winstead Terrace, Sunnyvale, CA 94087; email: connordukeg@mail.com.
[b] Department of Physics, Brigham Young University, Provo, UT 84602; email: scott_sommerfeldt@byu.edu.
[c] Department of Physics, Brigham Young University, Provo, UT 84602; email: kentgee@byu.edu.
[d] Department of Physics, Brigham Young University, Provo, UT 84602; email: coledukeg@mail.com.

Genetic algorithms have been used for optimization of control source and error sensor placement in a number of different active noise and vibration control applications. Many of these applications have involved enclosed sound fields[14–20]. However, in a free-field setting, Martin and Roure[21] were able to achieve 10–25 dB of sound pressure reduction at 100 Hz and 0–30 dB of sound pressure reduction at 200 Hz of an electronic transformer by the optimization of discrete control source locations in the near field of the primary source. In this paper, the principles of a value-based genetic algorithm are explored to find a control source configuration that will provide the greatest attenuation for a single primary source radiating into free space. Multiple studies have been performed to find a control source configuration that will provide the greatest attenuation for a single primary source radiating into free space.

2 THEORY OF SOUND POWER MINIMIZATION

Global free-field ANC is achieved by changing the radiation impedance of the primary source using secondary sources. In the case of fan noise, the fan is the primary noise source. Secondary or control sources are put in the near field of the primary source and, as they are driven by signals from the controller, create a mutual impedance upon the primary noise source[1,7,9].

The mutual impedance on one monopole source due to another monopole source is

$$Z(kd) = \frac{jk^2 \rho_o c}{4\pi}\left(\frac{e^{-jkd}}{kd}\right) \quad (1)$$

where k is the wave number, d is the distance between the two sources, ρ_o is the density of the radiation medium, c is the speed of sound in the medium.

Each source in the system, primary and control, affects the total power radiated by the system. The impedance created by each primary source on each other primary source can be written in complex matrix format $\bar{Z}_{pp}$, where Z_{12} is an element of $\bar{Z}_{pp}$ and represents the impedance created on the first primary source due to the presence of the second primary source and so forth. The effect of the control sources on each other can similarly be written, $\bar{Z}_{cc}$. The impedance "seen" by the primary sources due to the control sources and vice versa can be written $\bar{Z}_{pc}$ and $\bar{Z}_{cp}$, respectively. The total sound power radiated by the system is

$$\Pi = \frac{1}{2}\{\bar{Q}_p^H \,\mathrm{Re}[\bar{Z}_{pp}]\bar{Q}_p + \bar{Q}_c^H \,\mathrm{Re}[\bar{Z}_{pc}]\bar{Q}_p + \bar{Q}_p^H \,\mathrm{Re}[\bar{Z}_{cp}]\bar{Q}_c + \bar{Q}_c^H \,\mathrm{Re}[\bar{Z}_{cc}]\bar{Q}_c\}, \quad (2)$$

where $\bar{Q}_p$ and $\bar{Q}_c$ are complex column vectors of the source strengths of the primary and control sources, respectively[7–11]. If we define

$$\bar{A} = \frac{1}{2}\,\mathrm{Re}[\bar{Z}_{cc}], \quad (3)$$

$$\bar{B} = \frac{1}{2}\,\mathrm{Re}[\bar{Z}_{pc}]\bar{Q}_p, \quad (4)$$

and

$$C = \frac{1}{2}\bar{Q}_p^H \,\mathrm{Re}[\bar{Z}_{pp}]\bar{Q}_p, \quad (5)$$

the minimized power from the system, $\Pi_{\min}$, can be expressed as

$$\Pi_{\min} = C - \bar{B}^H \bar{A}^{-1} \bar{B}. \quad (6)$$

Optimal source strengths in complex matrix form for each control source, $\bar{Q}_{co}$, can be found using the equation

$$\bar{Q}_{co} = -\bar{A}^{-1}\bar{B}. \quad (7)$$

With the control sources of the system driven to these complex source strengths the minimized sound power field will be obtained[10,11]. The minimized sound power will depend upon the number of control sources, the configuration of the sources, and the frequency.

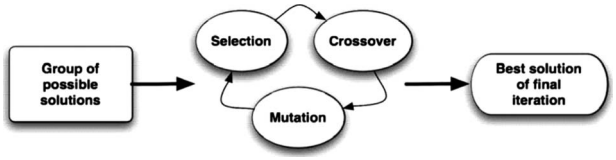

Fig. 1—Flow chart of typical genetic algorithm.

The optimization of a control source configuration to minimize radiated sound power cannot be generally done using conventional methods, such as gradient descent or Newton's method, due to the possible presence of many local optima, or configurations that are superior to nearby configurations in the variable space[22]. However, a genetic algorithm can be implemented to find a global optimum in a problem where many local minima exist.

3 GENETIC ALGORITHM

3.1 Basic Genetic Algorithm

Genetic algorithms use a selection of possible solutions that are combined and changed, in a process similar to natural selection, to find the best possible solution[22]. In problems where the variable space cannot be comprehensively investigated, genetic algorithms can investigate a large variable space efficiently. Gen and Cheng[23] state that there are 5 basic components to a genetic algorithm:

1—A genetic representation of solutions to the problem.

2—A way to create an initial population of solutions.

3—An evaluation function rating solutions in terms of fitness.

4—Genetic operators that alter the genetic composition of children during reproduction.

5—Values for parameters of genetic algorithms.

Configurations from an initial population of possible solutions are selected and are used to create a new group of possible solutions through a process called crossover, which mimics a genetic operation. The new group of possible solutions is randomly changed, adding diversity into the group of possible solutions. The best configuration is chosen from the final group of configurations as the optimum. The optimum found by the algorithm is based on probability and the specific type of processes used in the genetic algorithm[22]. The probability of finding the optimal solution of the system will increase with the number of iterations but no verification that the solution is a global optimum nor a meaningful quantitative probability can be obtained without an exhaustive search. A typical genetic algorithm is depicted in Fig. 1.

3.2 Genetic Algorithm Implementation

A value-based representation of the possible solutions was used in this algorithm. In most genetic algorithms a binary representation is used but does not have the resolution of a value-based representation. The limit in resolution originates from the conversion of the variables into a binary representation, a string of ones and zeros, while the value-based representation uses the numerical value. In this implementation, high resolution was important to find the optimal solution that could exist close to infeasible solutions or local optima. Each possible solution was ranked by the theoretical sound power attenuation that could be achieved. Constraints were added to the algorithm to include practical issues, including source size. The algorithm is not able to place two sources, primary or control, closer than the physical dimensions will allow. If the algorithm makes a configuration that violates these constraints, a new configuration that meets the constraints replaces the invalid solution. Both control and primary sources were modeled as simple monopoles, similar to work by Gee and Sommerfeldt[1].

The selection process is based on probability. The configurations with better achievable attenuation have a greater probability of being used to create the new group of configurations. Typical types of blend crossover for a value-based genetic algorithm could not be used in this situation. The blend crossover takes two possible configurations and combines them to create a new configuration[22]. If there is an infeasible space, i.e. an area where objects cannot be placed, close to the optimal configuration, the blend crossover can create entire iterations with infeasible configurations. To avoid this, a modified crossover process was developed for a real-value based genetic algorithm, which we referred to as "parthenogenesis."[1)] By using the natural concept of parthenogenesis, a single configuration can be perturbed to create a similar, but not identical, configuration rather than using two configurations to produce a new possible configuration. Katayama and Narihisa used a similar principle for binary based genetic algorithms and their implementation was found to give desirable results[24].

A possible configuration consisted of an array of values, each value representing a coordinate in space for a single control source. Possible configurations were initiated randomly. Constraints of the system were introduced by allowing the user to define the size of the search space as well as the physical dimensions of each source. If a configuration did not meet the constraints of the system, each source within the search space as well as the physical spacing of the sources, the configuration was replaced. The fitness of each configuration was determined by calculating the sound power of each configuration and the possible configurations were ranked based on this fitness.

The tournament selection process was used to determine which possible configurations would be used in the parthenogenesis crossover method. In tournament selection possible solutions compete against each other and the possible solution with the lowest radiated sound power advances to the next round. This was done until two possible solutions remained. Two solutions were selected rather than a single solution to allow for more diversity in the population.

The two possible solutions from the selection process were used in the parthenogenesis crossover technique to create a new group of possible solutions. This is done by taking a random number that is normally distributed around zero, r_n, with a user defined standard deviation. The larger the standard deviation of r_n, the more the new configuration will be different relative to the parent. The random number is used to make a new configuration by the equation

$$y = \alpha r_n + x, \tag{8}$$

where x is the selected possible solution, y is the new possible solution, and α is a dynamic factor which varies the amount of change of each generation. The dynamic factor is

$$\alpha = \left(1 - \frac{n-1}{N}\right)^{\beta} \tag{9}$$

with n being the current generation, N the total number of generations, and β a user defined parameter which weights the dynamic nature of the function. The dynamic nature of the crossover allowed the algorithm to settle into the optimal solution with high precision. If new possible configurations based on the selected configuration did not meet the constraints of the system, the process was repeated until the constraints were met.

Dynamic mutation was introduced after crossover to introduce the needed diversity through changing randomly selected coordinates from possible configurations. If a single coordinate of a possible configuration, x, is selected to be mutated a random number, r_{mut}, is chosen, that is within the bounds of the variable space. If the random number is less than the coordinate, $r_{mut} \leqslant x$, the gene is mutated using the equation

[1)]The term "parthenogenesis" is a common biology term used to describe a type of asexual genetic operation or asexual reproduction found in many species where offspring does not share identical genetic characteristics as the progenitor.

$$x_{new} = x_{\min} + (r_{mut} - x_{\min})^{\alpha}(x - x_{\min})^{1-\alpha} \qquad (10)$$

The mutation can also be dynamic using the same dynamic factor, α, used in the parthenogenesis. The $x_{\min}$ variable is the minimum value that can be assigned to the specific gene. If $r_{mut} > x$ then the equation for the mutation is

$$x_{new} = x_{\max} - (x_{\max} - r_{mut})^{\alpha}(x_{\max} - x)^{1-\alpha}. \qquad (11)$$

The dynamic parthenogenesis crossover and dynamic mutation are very different in the probability of perturbation that the process introduces. The parthenogenesis perturbs the configuration in a way that is similar to the original configuration while the mutation process does not take the original configuration into account.

The dynamic nature forces the crossover and mutation to favor the current value of the gene as the current generation reaches the final generation. The new group of configurations was then used to repeat the process and the configuration with the highest fitness (i.e., the lowest sound power output) was the solution from the algorithm. The more iterations the algorithm was allowed to complete, the higher the probability of finding the global optimum of the system. The number of iterations used was based upon resources available for computation.

The variable space for this problem is particularly sensitive to control source placement as the control sources become close to the optimum. If the control sources are not near the optimum then the sound power output is not sensitive to changes in position. Sensitivity analysis does not give meaningful quantitative results without an exhaustive search of the variable space and a consistent path through the variable space. Genetic algorithms are used to avoid both of these cases.

3.3 Genetic Algorithm Results

3.3.1 Four control sources

The first test case considered with the genetic algorithm was that of four control sources and a single primary source. This test was to see if the symmetric arrangement of Gee and Sommerfeldt[1] was indeed optimal; or in other words, that four symmetrically oriented control sources around a primary source resulted in the minimum power output from the system. For this test, a 90-mm diameter primary source and 30-mm control sources were configured so as to achieve strong source coupling. The algorithm was constrained to only two dimensions in the plane of the fan, as was done by Gee and Sommerfeldt[1]. Since the amount of control is based on the distances between the sources, a symmetric configuration (see Fig. 2(a)) was thought to be the optimal configuration based on the

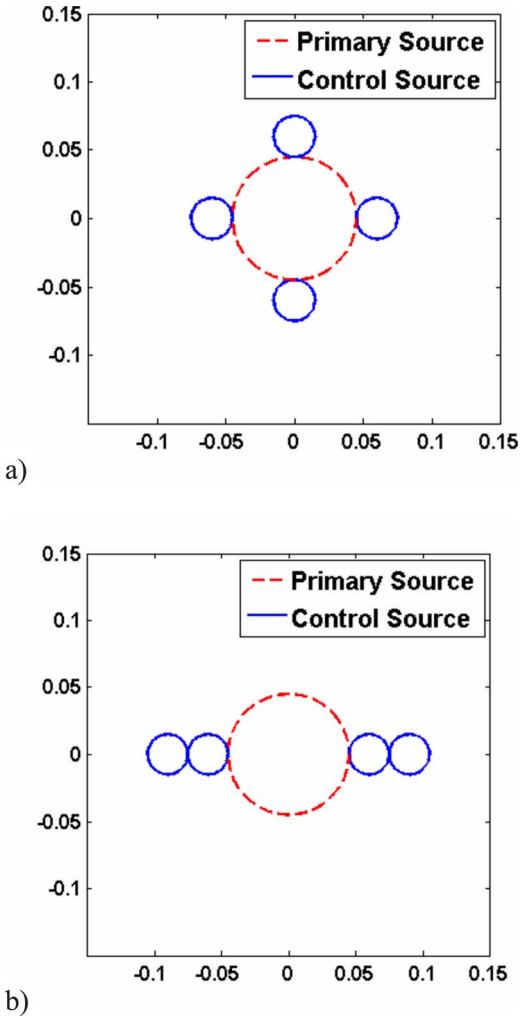

Fig. 2—a) Symmetric and b) linear control source configurations.

symmetric nature of the attenuation and the minimized distance between the primary source and each control source[1,9]. However, the solution given by the genetic algorithm is not the symmetrically distributed control sources, but rather the control sources in a linear configuration (see Fig. 2(b)). A comparison of the sound power with control, W_o, to the sound power with only primary sources, W_{pp}, from the two configurations can be seen in Fig. 3. The superior sound power attenuation from the linear configuration relative to the symmetric arrangement is not limited to a single frequency.

A closer look at Fig. 3 shows that at 500 Hz the linear configuration would be able to achieve about 30 dB more of sound power reduction (see Fig. 4(a)). This same amount of reduction is not seen for all frequency ranges, however. At higher frequencies, the symmetric case actually has better theoretical attenuation (see Fig. 4(b)), but this higher frequency range has such small possible attenuation that passive noise

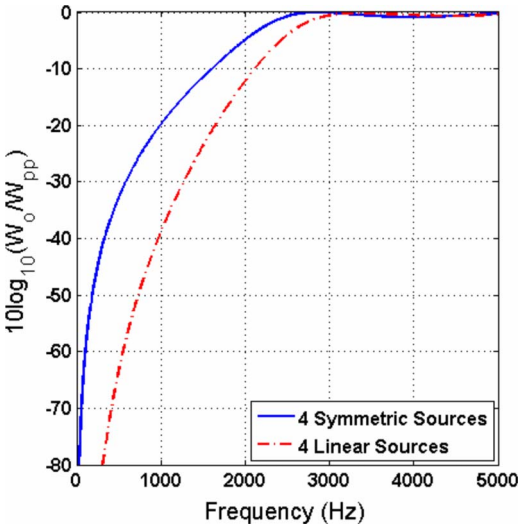

Fig. 3—Comparison of sound power attenuation for the symmetric and linear configurations as a function of frequency.

control techniques are better suited for the application. These results were also confirmed using the radiation mode technique.

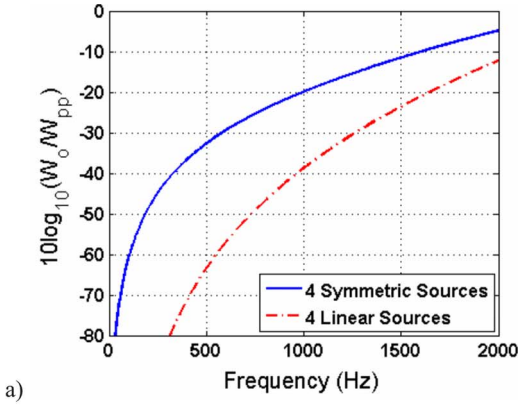

a)

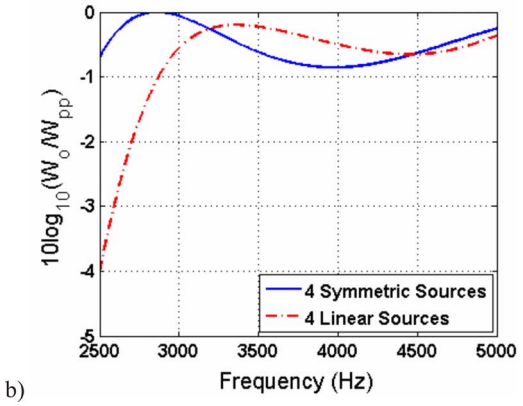

b)

Fig. 4—Zoomed plots for the comparison of sound power attenuation for the symmetric and linear configurations as a function of frequency.

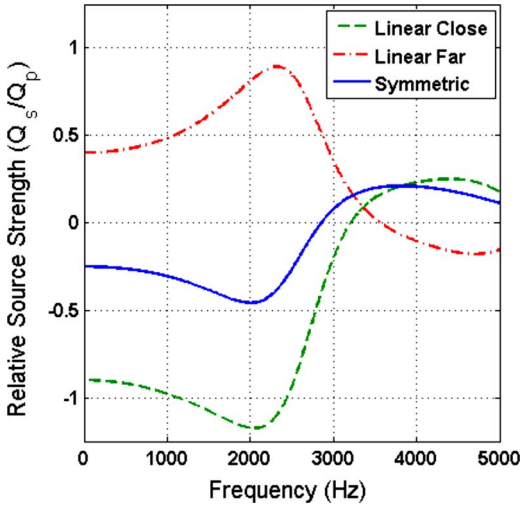

Fig. 5—Relative source strength of control sources for the linear and symmetric configurations as a function of frequency.

Another significant difference between the two configurations lies in the source strengths required from the control sources to create the minimized sound power field. If the required source strengths are too great, the physical control sources will be unable to match the source strength of the primary source without significant distortion being introduced. Figure 5 compares the relative source strength required from each control source for each configuration. There is a single curve for the symmetric source as the source strength required from each source is the same. The linear configuration has two unique curves, one for the sources closer to the primary source and one curve for the sources which are farther from the primary source. For the symmetric configuration the source strength of the control sources, Q_s, is never required to be higher than half of the source strength of the primary source, Q_p. In the linear configuration, however, the source strength of the two sources closest to the primary source are each required to have a relative source strength between 0.90 and 1.19 of the primary source for the frequency range of interest.

Allowing the algorithm to expand into a third dimension results in more possible configurations, although mounting control sources as such may be impractical for some scenarios. The algorithm demonstrated a tendency to converge to two different configurations, a linear and a tetrahedral configuration, shown in Fig. 6. The linear configuration has greater sound power attenuation then the tetrahedral configuration as shown in Fig. 7; consequently, the tetrahedral configuration would be considered a local minimum. For the algorithm to find the linear configuration consistently, a

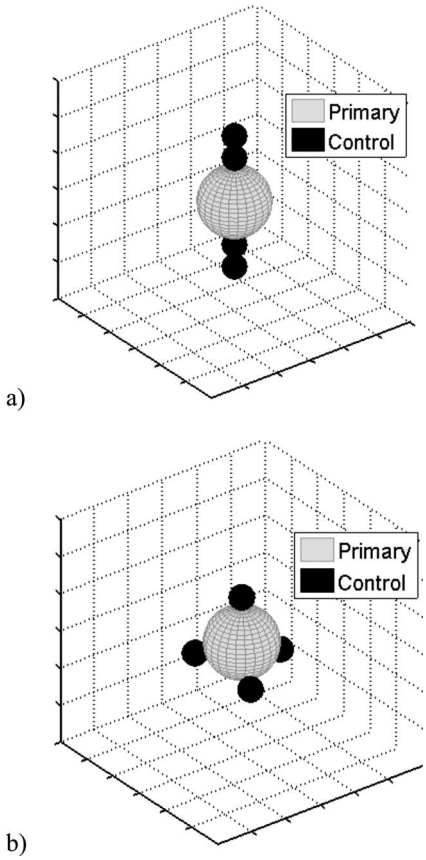

Fig. 6—a) Linear and b) tetrahedral configurations with four control sources and a single primary source in three dimensions.

higher mutation probability and larger generations size were necessary than the available resources would allow.

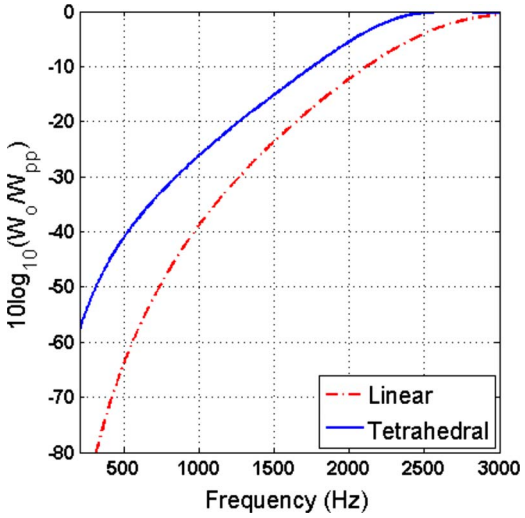

Fig. 7—Comparison of the sound power attenuation as a function of frequency for the linear and tetrahedral configurations.

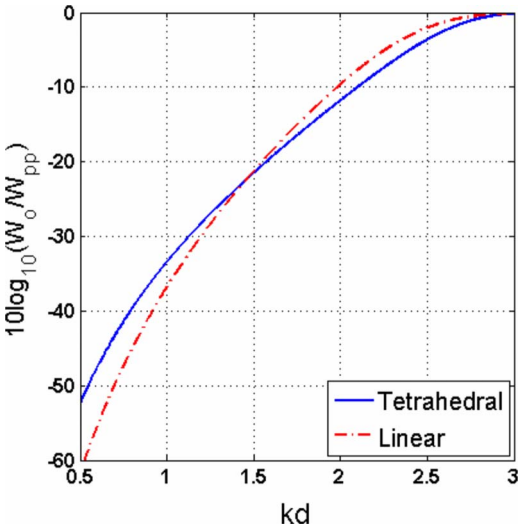

Fig. 8—Comparison of the sound power attenuation as a function of frequency for the linear and tetrahedral configurations using a single characteristic distance.

The superior attenuation achieved by the linear configuration, in both two and three dimensions, can be attributed to the smaller spacing between the control sources. If the physical size of the control sources is the same as the primary source, a characteristic distance, d, between sources can be used. A product of the wave number, k, and the characteristic distance can be used to calculate the theoretical maximum attenuation. In this case, the linear configuration achieves better sound power attenuation at lower frequencies while the tetrahedral configuration is better above a kd of 1.47 as is shown in Fig. 8.

In the low-frequency approximation, the radiation characteristics of the linear and tetrahedral arrangements show some significant differences. Nelson et al.[8] showed that the tetrahedral configuration radiates much like an octupole, proportional to $(kd)^6$. The linear configuration radiates as a higher order source, similar to that of $(kd)^8$. The slope of the power radiation of the two configurations (shown in Fig. 9 on a log scale) should be similar to the slope of a power of kd with which it shares radiation characteristics. The higher order source radiation explains why more attenuation is achieved with the linear configuration at low frequencies, even in three dimensions.

3.3.2 Six control sources

Similar procedures were followed for a single primary source with six control sources in three dimensions. Two control source configurations proved to be superior to other configurations, shown in Fig. 10. When control sources were required to be the same size

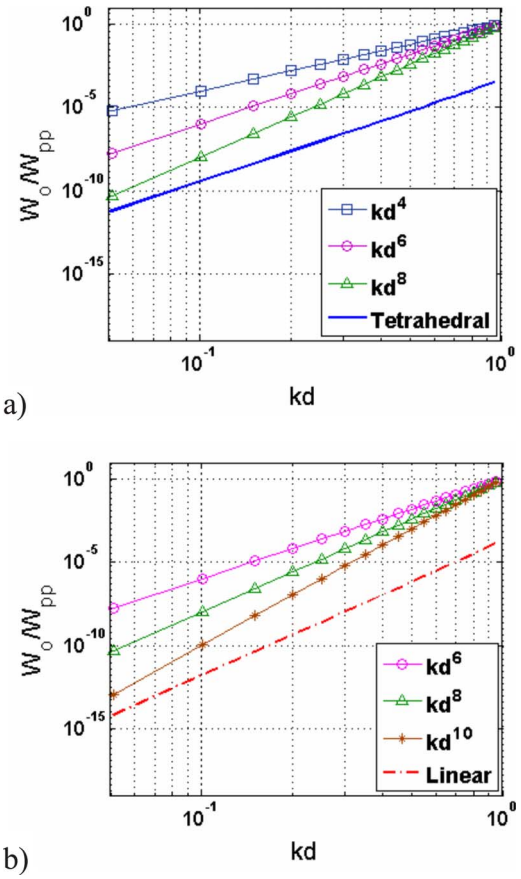

Fig. 9—Sound power radiation comparison in the low-frequency approximation to powers of kd for the a) tetrahedral and b) linear configurations.

as the primary source, and a single characteristic distance was used, the linear configuration again provided better reduction at low values of *kd*. However, Fig. 11 shows that the surrounding configuration yielded greater reduction for values of *kd* above 1.52. As with the four control source configuration in the previous subsection, when the control sources are smaller in diameter than the primary source, the attenuation from the linear configuration will become superior over a wider frequency range.

Radiation characteristics of the six control source configurations again exhibit significant differences in the low-frequency approximation. The radiation of the surrounding configuration goes as $(kd)^8$, similar to the four control sources in the optimal (linear) configuration. The six linear control sources radiate with $(kd)^{12}$ characteristics, as is shown in Fig. 12.

Source strength requirements for the six, linearly arranged control sources are similar to the four control source example. Figure 13 shows that the linear configuration requires greater source strengths from some of the control sources than the control sources in the surrounding, symmetrically oriented configuration.

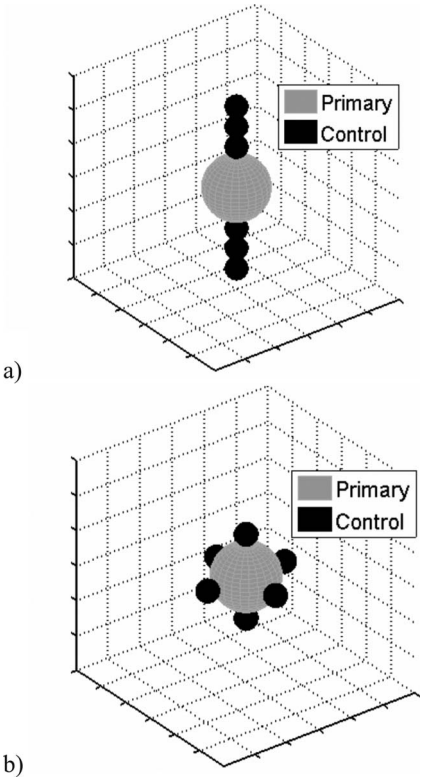

Fig. 10—a) Linear and b) surrounding configurations with six control sources and a single primary source in three dimensions.

The required source strength can be a limitation if the control actuators that are used cannot create the response needed to achieve the minimized sound power field. This becomes an issue when attempting to also minimize the size of the control sources so as to nearly collocate them with the primary source.

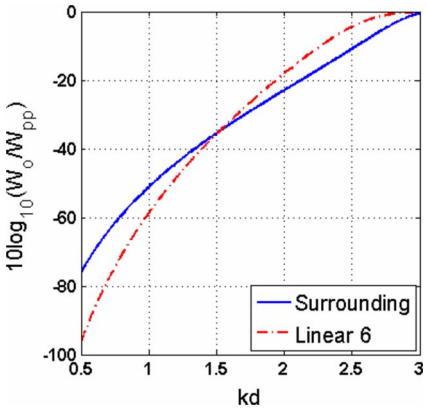

Fig. 11—Comparison of the sound power attenuation as a function of frequency for the linear and surrounding configurations with six control sources.

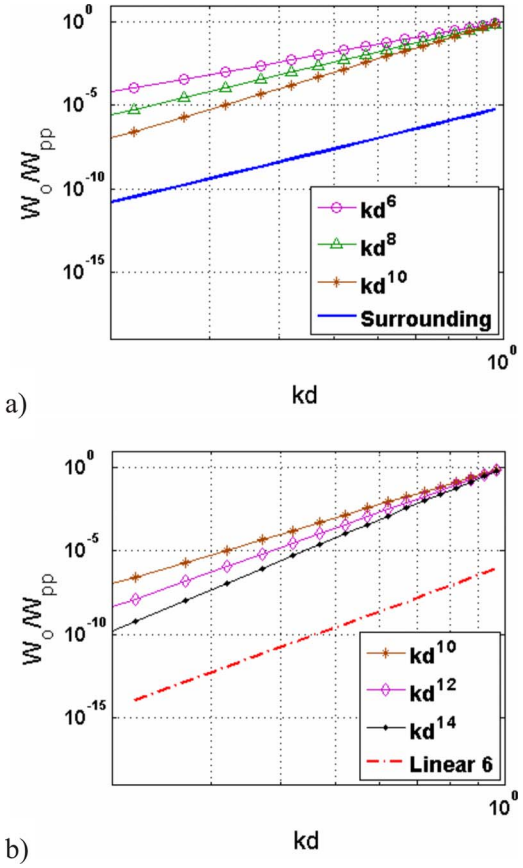

Fig. 12—Sound power radiation comparison in the low-frequency approximation to powers of kd for the a) surrounding and b) linear configurations with six control sources.

4 EXPERIMENTAL SETUP

Experimental verification of the genetic algorithm results was performed using loudspeakers mounted in

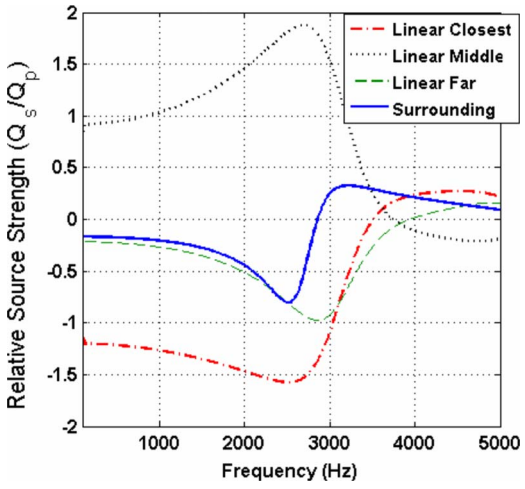

Fig. 13—Relative source strength of control sources for the linear and surrounding configurations with six control sources as a function of frequency.

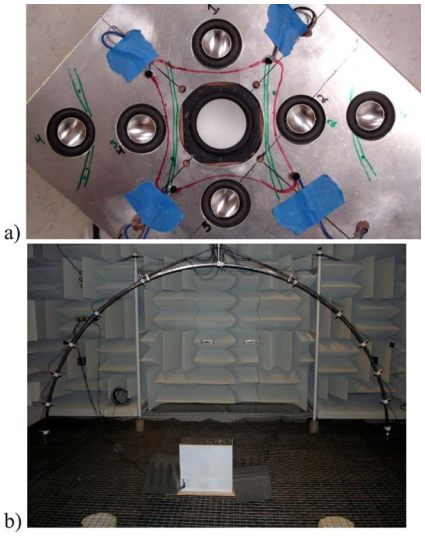

Fig. 14—Photographs of a) experimental plate with linear and symmetric control source arrangement and b) rotating microphone array in anechoic chamber.

an aluminum plate mounted in a mock computer enclosure. The primary source for the experiments was a single 50-mm diameter loudspeaker driven with a 550 Hz sawtooth waveform. Multiple 25-mm diameter loudspeakers were used as control sources in two different configurations, symmetric and linear as seen in Fig. 14(a). The limiting factors in placing these sources as close as possible were mounting fixtures and enclosures on the backside of the plate, requiring the 90 mm and 30 mm diameter values in the analysis.

A filtered-X algorithm was implemented using a 16-bit TI TMS320C6713GDP for signal processing. Signal conditioning was performed by using band-pass filters and variable gain stages on the reference, error sensor, and control source signals.

Acoustical measurements were taken using a 13-microphone array in an anechoic chamber displayed in Fig. 14(b). The microphone array was rotated around the aluminum plate setup in 10-degree increments to form a hemisphere. The radiated sound power of the system, at the frequency of interest, was calculated using the hemisphere of pressure data and assuming symmetry of the measured hemisphere and the unmeasured hemisphere. Figures 15 and 16 show the radiation from the symmetric and linear configurations, respectively, at three frequencies of interest. The mesh grid shows the sound pressure level, by distance from the center, in a given direction with no ANC system. The solid surface shows sound pressure level, by distance from the center and shade, when the ANC system is used. The sound power reduction for each configuration and frequency of interest is shown in the title of the

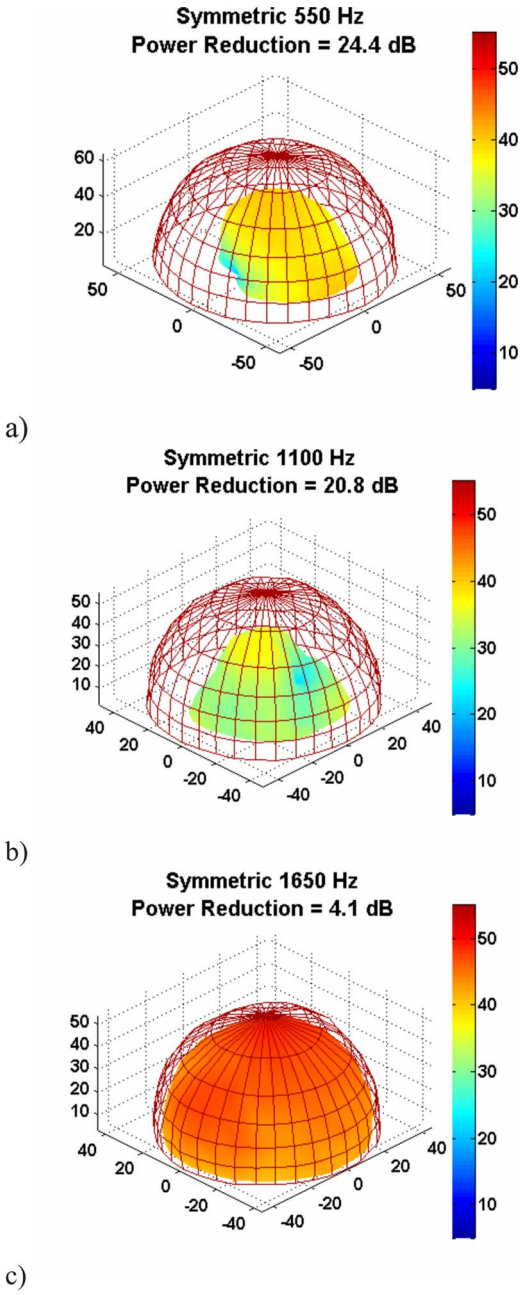

Fig. 15—Sound power reduction of four control sources configured symmetrically for a) 550 Hz*, b)* 1100 Hz*, and c)* 1650 Hz.

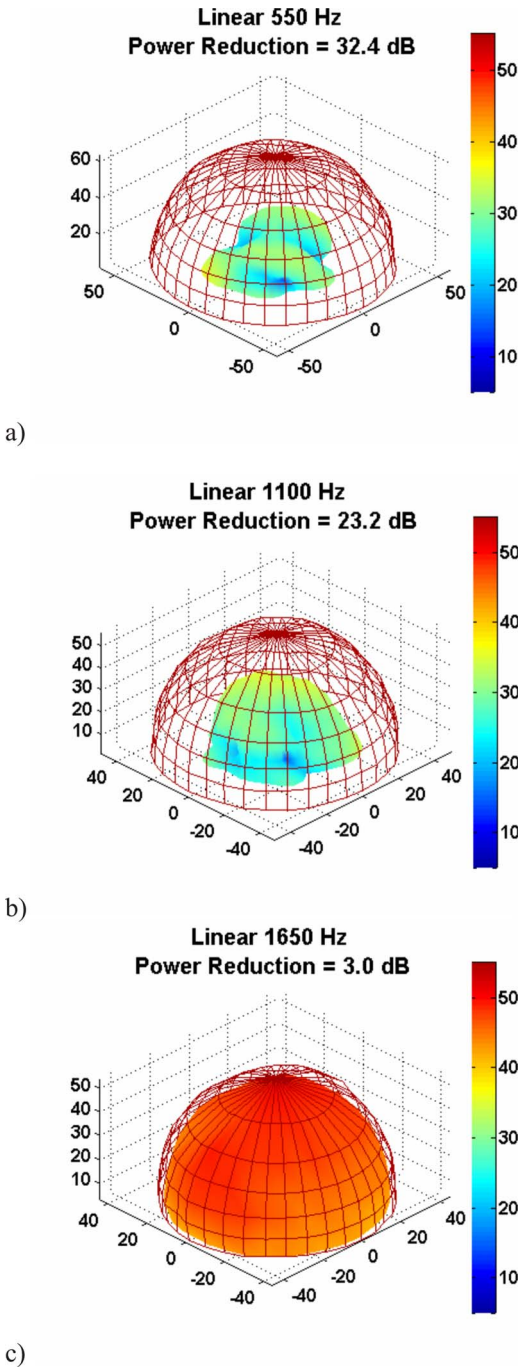

Fig. 16—Sound power reduction of four control sources configured linearly for a) 550 Hz*, b)* 1100 Hz*, and c)* 1650 Hz.

figure as well as in Table 1. The sound power reduction for a given configuration was found to be consistent over multiple trials with a standard deviation of less than 0.1 dB.

5 EXPERIMENTAL RESULTS

Both configurations achieved significant global reduction in radiated power for the first two harmonics. In each case the linear configuration outperformed the symmetric configuration. The third harmonic showed significantly less sound power reduction due to the control system's anti-aliasing filters that had a cutoff frequency of 1400 Hz. The experimental radiation is not symmetric due to the orientation of the sources relative to the mock computer enclosure.

Additional experiments were carried out with different fundamental frequencies of the primary sawtooth waveform, the purpose of which was to map out the performance of the two control source arrangements as a function of frequency. The different fundamental frequencies of the sawtooth waveform were 350 Hz, 450 Hz, 475 Hz, 525 Hz, 600 Hz, and 650 Hz. These

Table 1—Theoretical and experimental sound power attenuation (dB) for the symmetric and linear configuration at multiple frequencies of interest.

	550 Hz	1100 Hz	1650 Hz
Symmetric Configuration			
Theoretical	32.3	19.4	10.9
Experimental	24.4	20.8	4.1
Linear Configuration			
Theoretical	58.4	33.4	17.7
Experimental	32.4	23.2	3.0

frequencies were chosen to have minimal aliasing effects with the 2 kHz Nyquist frequency. The attenuation as a function of the fundamental and harmonics is shown in Fig. 17 along with the theoretical attenuation curves attained when each source is modeled as a point monopole. In the frequency range from 500 to 1300 Hz, the linear configuration did significantly better than the symmetric configuration. The amount of attenuation achieved by the linear configuration did not reach the theoretical limit, which may be due to the error sensor placement, achievable control source strength, and accuracy of control source placement. Although the error sensors were placed in the theoretical pressure nulls, optimization techniques for the error sensor placement along theoretical nulls may increase the experimental attenuation for the linear configuration[25–27]. Reduced attenuation at high and low-frequency bands are due to other effects. Low-frequency attenuation was limited by the control actuators' response. Above 1400 Hz, the anti-aliasing filters used in the ANC system limited the amount of attenuation achieved.

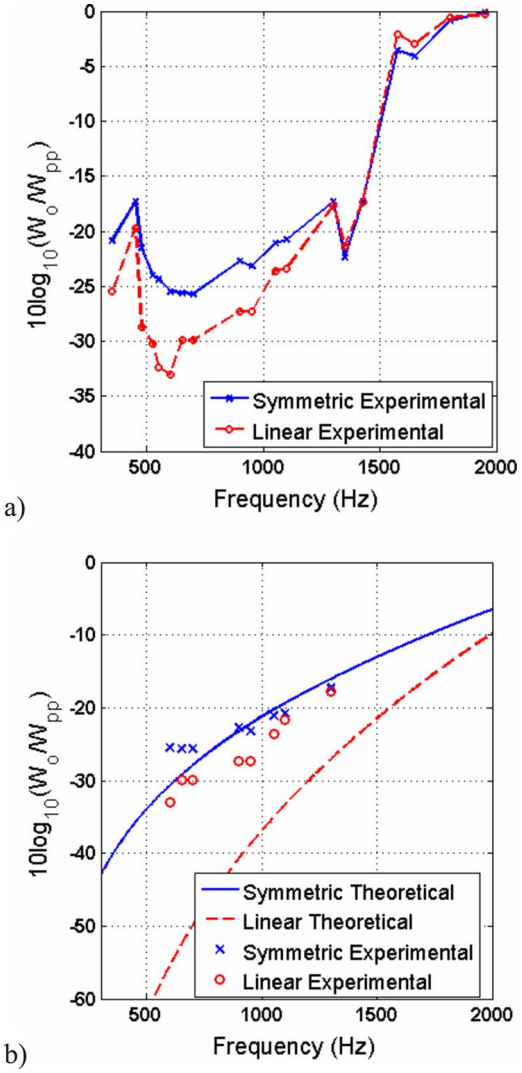

Fig. 17—Comparison of the a) experimental and the b) theoretical attenuation as a function of frequency for the symmetric and linear configurations.

6 CONCLUSIONS

A genetic algorithm can be used to find the optimal source configuration in ANC applications. When using four control sources and a single primary source radiating into free space, the best sound power attenuation will be achieved by using a linear configuration rather than a symmetric configuration. Expanding the genetic algorithm to include three-dimensional configurations has also revealed that a linear configuration is superior to other configurations at low frequencies. At higher frequency ranges, the tetrahedral configuration will allow more sound power attenuation if the control sources are the same size or bigger than the primary source. Similar results were found using six control sources. Experimental data confirmed that the linear configuration of control sources achieves better attenuation than other control source configurations.

7 REFERENCES

1. K. L. Gee and S. D. Sommerfeldt, "Application of theoretical modeling to multichannel active control of cooling fan noise", *J. Acoust. Soc. Am.*, **115**, 228–236, (2004).
2. A. Gerard, A. Berry and P. Masson, "Control of tonal noise from subsonic axial fan. Part 2: Active control simulations and experiments in free field", *J. Sound Vib.*, **288**, 1077–1104, (2005).
3. G. C. Lauchle, J. R. MacGillivray and D. C. Swanson, "Active control of axial-flow fan noise", *J. Acoust. Soc. Am.*, **101**, 341–349, (1997).
4. D. A. Quinlan, "Application of active control to axial flow fans", *Noise Control Eng. J.*, **39**, 95–101, (1992).
5. B. T. Wang, "Optimal placement of microphones and piezoelectric transducer actuators for far-field sound radiation control", *J. Acoust. Soc. Am.*, **99**, 2975–2984, (1996).
6. S. D. Snyder, "Microprocessors for active control: Bigger is not always better", *Proceedings of ACTIVE 99*, Fort Lauderdale, FL,

Noise Control Foundation, Poughkeepsie, NY, pp. 45–62, (1999).
7. C. H. Hansen and S. D. Snyder, *Active Control of Noise and Vibration*, E & FN SPON, London, (1997).
8. P. A. Nelson, A. R. D. Curtis, S. J. Elliott and A. J. Bullmore, "The minimum power output of free field point sources and the active control of sound", *J. Sound Vib.*, **116**, 397–414, (1987).
9. P. A. Nelson and S. J. Elliot, *Active Control of Sound*, Academic, London, p. 436, (1992).
10. M. E. Johnson and S. J. Elliot, "Measurement of acoustic power output in the active control of sound", *J. Acoust. Soc. Am.*, **93**, 1453–1459, (1993).
11. S. J. Elliot, P. Joseph, P. A. Helson and M. E. Johnson, "Power output minimization and power absorption in the active control of sound", *J. Acoust. Soc. Am.*, **90**, 2501–2512, (1991).
12. K. A. Cunefare, M. N. Currey, M. E. Johnson and S. J. Elliott, "The radiation efficiency grouping of free space acoustic radiation modes", *J. Acoust. Soc. Am.*, **109**, 203–215, (2001).
13. S. J. Elliot and M. E. Johnson, "Radiation modes and the active control of sound power", *J. Acoust. Soc. Am.*, **94**, 2194–2204, (1993).
14. Z. G. Diamantis, D. T. Tsahalis and I. Borchers, "Optimization of an active noise control system inside an aircraft, based on the simultaneous optimal positioning of microphones and speakers, with the use of a genetic algorithm", *Comput. Optim. Appl.*, **23**, 65–76, (2002).
15. S. J. Elliot, P. A. Nelson, I. M. Stothers and C. C. Boucher, "In-flight experiments on the active control of propeller-induced cabin noise", *J. Sound Vib.*, **140**, 219–238, (1990).
16. D. S. Li and M. Hodgson, "Optimal active noise control in large rooms using a 'locally global' control strategy", *J. Acoust. Soc. Am.*, **118**, 3653–3661, (2005).
17. D. S. Li, L. Cheng and C. M. Gosselin, "Optimal design of PZT actuators in active structural acoustic control of a cylindrical shell with a floor partition", *J. Sound Vib.*, **269**, 569–588, (2004).
18. D. A. Manolas, I. Borchers and D. T. Tsahalis, "Simulataneous optimization of the sensor and actuator positions for an active noise and/or vibration control system using genetic algorithms, applied in a Donier aircraft", *Eng. Comput.*, **17**, 620–630, (2000).
19. S. Pottie and D. Botteldooren, "Optimal placement of secondary sources for active noise control using a genetic algorithm", *Proceedings of Inter-Noise 96*, Liverpool, UK, Noise Control Foundation, Poughkeepsie, NY, pp. 1101–1104, (1996).
20. M. T. Simpson and C. H. Hansen, "Use of genetic algorithms to optimize vibration actuator placement for active control of harmonic interior noise in a cylinder with floor structure", *Noise Control Eng. J.*, **44**, 169–184, (1996).
21. T. Martin and A. Roure, "Active noise control of acoustic sources using spherical harmonics expansion and a genetic algorithm: Simulation and experiment", *J. Sound Vib.*, **212**, 511–523, (1998).
22. D. E. GoldBerg, *Genetic Algorithms in Search, Optimization, and Machine Learning*, Addison-Wesley Publishing Company Inc., Reading, Massachusetts, p. 412, (1998).
23. M. Gen and R. Cheng, *Genetic Algorithms and Engineering Optimization*, John Wiley and Sons Inc., New York, New York, (2000).
24. K. Katayama and H. Narihisa, "On fundamental design of parthenogenetic algorithm for the binary quadratic programming problem", *Proc. 2001 Congress on Evolutionary Computation*, Seoul, Korea, IEEE, Piscataway, NJ, pp. 356–363, (2001).
25. B. M. Shafer, K. L. Gee, S. D. Sommerfeldt and C. V. Duke, "Near-field mapping of pressure fields during active noise control of small axial cooling fans", *J. Acoust. Soc. Am.*, **120**, 3198, (2006).
26. B. M. Shafer, K. L. Gee, S. D. Sommerfeldt and J. I. Fjeldsted, "Determination of optimal near-field error sensor locations for active control of cooling fan noise using spherical harmonic expansions", *J. Acoust. Soc. Am.*, **121**, 3180, (2007).
27. K. L. Gee and S. D. Sommerfeldt, "A compact active control implementation for axial cooling fan noise", *Noise Control Eng. J.*, **51**, 325–334, (2003).